Synchronization of chaotic oscillator time scales

Alexander E. Hramov,[1,*] Alexey A. Koronovskii,[1] and Yurij I. Levin[1]

[1]*Department of Nonlinear Processes, Saratov State University, Astrakhanskaya, 83, Saratov, 410012, Russia*

(Dated: February 8, 2008)

Abstract

This paper deals with the chaotic oscillator synchronization. A new approach to detect the synchronized behaviour of chaotic oscillators has been proposed. This approach is based on the analysis of different time scales in the time series generated by the coupled chaotic oscillators. It has been shown that complete synchronization, phase synchronization, lag synchronization and generalized synchronization are the particular cases of the synchronized behavior called as "time–scale synchronization". The quantitative measure of chaotic oscillator synchronous behavior has been proposed. This approach has been applied for the coupled Rössler systems.

PACS numbers: 05.45.Xt, 05.45.Tp

*Electronic address: aeh@cas.ssu.runnet.ru

Introduction

Synchronization of chaotic oscillators is one of the fundamental phenomena of nonlinear dynamics. It takes place in many physical [1, 2, 3, 4, 5, 6] and biological [7, 8, 9] processes. It seems to play an important role in the ability of biological oscillators, such as neurons, to act cooperatively [10, 11, 12].

There are several different types of synchronization of coupled chaotic oscillators which have been described theoretically and observed experimentally [13, 14, 15, 16]. The *complete synchronization* (CS) implies coincidence of states of coupled oscillators $\mathbf{x}_1(t) \cong \mathbf{x}_2(t)$, the difference between state vectors of coupled systems converges to zero in the limit $t \to \infty$, [17, 18, 19, 20]. It appears when interacting systems are identical. If the parameters of coupled chaotic oscillators slightly mismathch, the state vectors are close $|\mathbf{x}_1(t) - \mathbf{x}_2(t)| \approx 0$, but differ from each other. Another type of synchronized behavior of coupled chaotic oscillators wihth slightly mismatched parameters is the *lag synchronization* (LS), when shifted in time, the state vectors coincide with each other, $\mathbf{x}_1(t + \tau) = \mathbf{x}_2(t)$. When the coupling between oscillator increases the time lag τ decreases and the synchronization regime tends to be CS one [21, 22, 23]. The *generalized synchronization* (GS) [24, 25, 26] introduced for drive–responce systems, means that there is some functional relation between coupled chaotic oscillators, i.e. $\mathbf{x}_2(t) = \mathbf{F}[\mathbf{x}_1(t)]$.

Finally, it is necessary to mention the *phase synchronization* (PS) regime. To describe the phase synchronization the instantaneous phase $\phi(t)$ of a chaotic continuous time series is usually introduced [13, 14, 15, 16, 27, 28]. The phase synchronization means the entrainment of phases of chaotic signals, whereas their amplitudes remain chaotic and uncorrelated.

All synchronization types mentioned above are associated with each other (see for detail [1, 22, 24]), but the relationship between them is not completely clarified yet. For each type of synchronization there are their own ways to detect the synchronized behavior of coupled chaotic oscillators. The complete synchronization can be displayed by means of comparison of system state vectors $\mathbf{x}_1(t)$ and $\mathbf{x}_2(t)$, whereas the lag synchronization can be determined by means of the similarity function [21]. The case of the generalized synchronization is more intricate because the functional relation $\mathbf{F}[\cdot]$ can be very complicated, but there are several methods to detect the synchronized behavior of coupled chaotic oscillators, such as the auxiliary system approach [29] or the method of nearest neighbors [24, 30].

Finally, the phase synchronization of two coupled chaotic oscillators occurs if the difference between the instantaneous phases $\phi(t)$ of chaotic signals $\mathbf{x}_{1,2}(t)$ is bounded by some constant

$$|\phi_1(t) - \phi_2(t)| < \text{const.} \tag{1}$$

It is possible to define a mean frequency of chaotic signal

$$\bar{\Omega} = \lim_{t\to\infty} \frac{\phi(t)}{t} = \langle \dot{\phi}(t) \rangle, \tag{2}$$

which should be the same for both coupled chaotic systems, i.e., the phase locking leads to the frequency entrainment. It is important to notice, to obtain correct results the mean frequency $\bar{\Omega}$ of chaotic signal $\mathbf{x}(t)$ should coincide with the main frequency $\Omega_0 = 2\pi f_0$ of the Fourier spectrum (for detail, see [31]). There is no general way to introduce the phase for chaotic time series. There are several approaches which allow to define the phase for "good" systems with simple topology of chaotic attractor (so–called "phase coherent attractor"), the Fourier spectrum of which contains the single main frequency f_0.

First of all, the plane in the system phase space may exist, on which the projection of the chaotic attractor looks like circular band. For such plane the coordinates x and y can be introduced, the origin of this coordinate system should be placed somewhere near the center of the chaotic attractor projection. In this case the phase can be introduced as an angle in considered coordinate system [21, 32], but for that all trajectories of chaotic attractor projection on the (x, y)–plane should revolve around the origin. Sometimes, a coordinate transformation can be used to obtain a proper projection [13, 32]. One can also use the velocities $\dot{x}$ and $\dot{y}$, if the projections of chaotic trajectories on the plane $(\dot{x}, \dot{y})$ always rotate around the origin and in some cases this approach is more suitable [33, 34]. Another way to define the phase $\phi(t)$ of chaotic time series $x(t)$ is the constructing of the analytical signal [14, 27] using the Hilbert transform. Moreover, the Poincaré secant surface can be used for the introducing of the instantaneous phase of chaotic dynamical system [14, 27]. Finally, the phase of chaotic time series can be introduced by means of the continuous wavelet transform [35], but the appropriate wavelet function and its parameters should be chosen [36].

All these approaches give correct results for "good" systems with well–defined phase, but fail for oscillators with non-revolving trajectories. Such chaotic oscillators are often called as "systems with ill–defined phase". The phase introducing based on the approaches mentioned

above for the system with ill–defined phase leads usually to incorrect results [31]. Therefore, the phase synchronization of such systems can be usually detected by means of the indirect indications [32, 37] and measurements [33].

In this paper we propose a new approach to detect the synchronization between two coupled chaotic oscillators. The main idea of this approach consists in the analysis of the system behavior on different time scales that allows us to consider different cases of synchronization from the universal positions [38]. Using the continuous wavelet transform [39, 40, 41, 42] we introduce the continuous set of time scales s and associated with them instantaneous phases $\phi_s(t)$. (In other words, $\phi_s(t)$ is continuous function of time t and time scale s). As we will show further, if two chaotic oscillators demonstrate any type of synchronized behavior mentioned above (CS, LS, PS or GS), in the time series $\mathbf{x}_{1,2}(t)$ generated by these systems there are time scales s necessarily correlated for which the phase locking condition

$$|\phi_{s1}(t) - \phi_{s2}(t)| < \mathrm{const} \tag{3}$$

is satisfied. In other words, CS, LS, PS and GS are the particular cases of the synchronous coupled chaotic oscillator behavior called as *"time–scale synchronization"* (TSS).

The structure of this paper is the following. In section I we discuss the continuous wavelet transform and the method of the time scales s and associated with them phases $\phi_s(t)$ definition. In section II we consider the case of the phase synchronization of two mutually coupled Rössler systems. We demonstrate the application of our method and discuss the relationship between our and traditional approaches. Section III deals with the synchronization of two mutually coupled Rössler systems with funnel attractors. In this case the traditional methods for phase introducing fail and there is no possibility to detect the phase synchronization regime, respectively. The synchronization between systems can be revealed here only by means of the indirect measurements (see for detail [33]). We demonstrate the efficiency of our method for such cases and discuss the correlation between PS, LS and CS. In section IV we consider application of our method for the unidirectional coupled Rössler systems when the generalized synchronization is observed. The quantitative measure of synchronization is described in section V. The final conclusion is presented in section VI.

I. CONTINUOUS WAVELET TRANSFORM

The continuous wavelet transform is the powerful tool for the analysis of nonlinear dynamical system behavior. In particular, the continuous wavelet analysis has been used for the detection of synchronization of chaotic oscillations in the brain [35, 43, 44] and chaotic laser array [45]. It has also been used to detect the main frequency of the oscillations in nephron autoregulation [46]. We propose to analyze the dynamics of coupled chaotic oscillators using the consideration of system behavior on different time scales s each of them is characterized by means of its own phase $\phi_s(t)$, respectively. So, in order to define *the continuous set of instantaneous phases* $\phi_s(t)$ the continuous wavelet transform is the convenient mathematical tool.

Let us consider continuous wavelet transform of chaotic time series $x(t)$

$$W(s,t_0)=\int\limits_{-\infty}^{+\infty} x(t)\psi^*_{s,t_0}(t)\,dt, \tag{4}$$

where $\psi_{s,t_0}(t)$ is the wavelet–function related to the mother–wavelet $\psi_0(t)$ as

$$\psi_{s,t_0}(t)=\frac{1}{\sqrt{s}}\psi\left(\frac{t-t_0}{s}\right). \tag{5}$$

The time scale s corresponds to the width of the wavelet function $\psi_{s,t_0}(t)$, and t_0 is shift of wavelet along the time axis, the symbol "$*$" in (4) denotes complex conjugation. It should be noted that the time scale s is usually used instead of the frequency f of Fourier transformation and can be considered as the quantity inversed to it.

The Morlet–wavelet [47]

$$\psi_0(\eta)=\frac{1}{\sqrt[4]{\pi}}\exp(j\Omega_0\eta)\exp\left(\frac{-\eta^2}{2}\right) \tag{6}$$

has been used as a mother–wavelet function. The choice of parameter value $\Omega_0=2\pi$ provides the relation $s=1/f$ between the time scale s of wavelet transform and frequency f of Fourier transformation.

The wavelet surface

$$W(s,t_0)=|W(s,t_0)|e^{j\phi_s(t_0)} \tag{7}$$

describes the system's dynamics on every time scale s at the moment of time t_0. The value of $|W(s,t_0)|$ indicates the presence and intensity of the time scale s mode in the time series

$x(t)$ at the moment of time t_0. It is possible to consider the quantities

$$E(s,t_0) = |W(s,t_0)|^2 \tag{8}$$

and

$$\langle E(s)\rangle = \int |W(s,t_0)|^2\,dt_0, \tag{9}$$

which are instantaneous and integral energy distributions on time scales, respectively.

At the same time, the phase $\phi_s(t) = \arg W(s,t)$ is naturally introduced for every time scale s. It means that it is possible to describe the behavior of each time scale s by means of its own phase $\phi_s(t)$. If two interacting chaotic oscillators are synchronized it means that in time series $\mathbf{x}_1(t)$ and $\mathbf{x}_2(t)$ there are scales s correlated with each other. To detect such correlation one can examine the condition (3) which should be satisfied for synchronized time scales.

II. PHASE SYNCHRONIZATION OF TWO RÖSSLER SYSTEMS

Let us start our consideration with two mutually coupled Rössler systems with slightly mismatched parameters [27, 28]

$$\begin{aligned}
\dot{x}_{1,2} &= -\omega_{1,2}y_{1,2} - z_{1,2} + \varepsilon(x_{2,1} - x_{1,2}),\\
\dot{y}_{1,2} &= \omega_{1,2}x_{1,2} + ay_{1,2},\\
\dot{z}_{1,2} &= p + z_{1,2}(x_{1,2} - c),
\end{aligned} \tag{10}$$

where $a = 0.165$, $p = 0.2$, and $c = 10$. The parameters $\omega_{1,2} = \omega_0 \pm \Delta$ determine the parameter mistuning, ε is the coupling parameter ($\omega_0 = 0.97$, $\Delta = 0.02$). In [21] it has been shown that for these control parameter values and coupling parameter $\varepsilon = 0.05$ the phase synchronization is observed.

For this case the phase of chaotic signal can be easily introduced in one of the ways mentioned above, because the phase coherent attractor with rather simple topological properties is realized in the system phase space. The attractor projection on the (x, y)–plane resembles the smeared limit cycle where the phase point always rotates around the origin (Fig. 1,a). The Fourier spectrum $S(f)$ contains the main frequency peak $f_0 \simeq 0.163$ (see Fig. 1,b) which coincides with the mean frequency $\bar{f} = \bar{\Omega}/2\pi$, determined from the instantaneous phase $\phi(t)$ dynamics (2). Therefore, there are no complications to detect the

phase synchronization regime in two coupled Rössler systems (10) by means of traditional approaches.

When the coupling parameter ε is equal to 0.05 the phase synchronization between chaotic oscillators is observed. The phase locking condition (1) is satisfied and the mean frequencies $\bar{\Omega}_{1,2}$ are entrained. So, the time scales $s_0 \simeq 6$ of both chaotic systems corresponding to the mean frequencies $\bar{\Omega}_{1,2}$ should be correlated with each other. Correspondingly, the phases $\phi_{s1,2}(t)$ associated with these time scales s should be locked and the condition (3) should be satisfied. The time scales which are the nearest to the time scale s_0 should also be correlated, but the interval of the correlated time scales depends upon the coupling strength. At the same time, there should be time scales which remain uncorrelated. These uncorrelated time scales cause the difference between chaotic oscillations of coupled systems.

Figure 2 illustrates the behavior of different time scales for two coupled Rössler systems (10) with phase coherent attractors. It is clear, that the phase difference $\phi_{s1}(t) - \phi_{s2}(t)$ for scales $s_0 = 6$ is bounded and therefore time scales $s_0 = 6$ corresponding to the main frequency of Fourier spectrum f_0 are synchronized. It is important to note that wavelet power spectra $\langle E_{1,2}(s) \rangle$ close to each other (see Fig. 2,a) and time scales s characterized by the large value of energy (e.g., s=5) close to the main time scale $s_0 = 6.0$ are correlated, too. There are also time scales which are not synchronized, like $s = 3.0$, $s = 4.0$, etc. (see Fig. 2,b).

So, the phase synchronization of two mutually coupled chaotic oscillators with phase coherent attractors manifests itself as synchronous behavior of the time scales s_0 (and time scales s close to s_0) corresponding to the chaotic signal mean frequency $\bar{\Omega}$.

III. SYNCHRONIZATION OF TWO RÖSSLER SYSTEMS WITH FUNNEL ATTRACTORS

Let us consider the more complicated example when it is impossible to correctly introduce the instantaneous phase $\phi(t)$ of chaotic signal $\mathbf{x}(t)$. It is clear, that for such cases the traditional methods of the phase synchronization detecting fail and it is necessary to use the other techniques, e.g., indirect measurements [33]. On the contrary, our approach gives correct results and allows to detect the synchronization between chaotic oscillators as easily as before.

To illustrate it we consider two non–identical coupled Rössler systems with funnel attractors (Fig. 3):

$$\begin{aligned}\dot{x}_{1,2} &= -\omega_{1,2}y_{1,2} - z_{1,2} + \varepsilon(x_{2,1} - x_{1,2}),\\ \dot{y}_{1,2} &= \omega_{1,2}x_{1,2} + ay_{1,2} + \varepsilon(y_{2,1} - y_{1,2}),\\ \dot{z}_{1,2} &= p + z_{1,2}(x_{1,2} - c),\end{aligned} \tag{11}$$

where ε is a coupling parameter, $\omega_1 = 0.98$, $\omega_2 = 1.03$. The control parameter values have been selected by analogy with [33] as $a = 0.22$, $p = 0.1$, $c = 8.5$. It is necessary to note that under these control parameter values none of the methods mentioned above permits to define phase of chaotic signal correctly in whole range of coupling parameter ε variation. Therefore, nobody can determine by means of direct measurements whether the synchronization regime takes place for several values of parameter ε. On the contrary, our approach allows to detect synchronization between considered coupled oscillators easily for all values of coupling parameter.

In [33] it has been shown by means of the indirect measurements that for the coupling parameter value $\varepsilon = 0.05$ the synchronization of two mutually coupled Rössler systems (11) takes place. Our approach based on the analysis of the dynamics of different time scales s gives analogous results. So, the behavior of the phase difference $\phi_{s1}(t) - \phi_{s2}(t)$ for this case has been presented in figure 4,b. One can see that the phase locking takes place for the time scales $s = 5.25$ which are characterized by the largest energy value in the wavelet power spectra $\langle E(s)\rangle$ (see Fig. 4,a).

It is important to note that the phase difference $\phi_{s1}(t) - \phi_{s2}(t)$ is also bounded on the time scales close to $s = 5.25$. So, we can say that the time scales $s = 5.25$ (and close to them) of two oscillators are synchronized with each other. At the same time the other time scales (e.g., $s = 4.5, 6.0$ et. al.) remain uncorrelated. For such time scales the phase locking has not been observed (see Fig. 4,b).

It is clear, that the mechanism of the synchronization of coupled chaotic oscillators is the same in both cases considered in sections II and III. The synchronization phenomenon is caused by the existence of time scales s in system dynamics correlated with each other. Therefore, there is no reason to divide the considered synchronization examples into different types.

It has been shown in [21] that there is certain relationship between PS, LS and CS for chaotic oscillators with slightly mismatched parameters. With the increase of coupling

strength the systems undergo the transition from unsynchronized chaotic oscillations to the phase synchronization. With a further increase of coupling the lag synchronization is observed. Further increasing of the coupling parameter leads to the decreasing of the time lag and both systems tend to have the complete synchronization regime.

Let us consider the dynamics of different time scales s of two nonidentical mutually coupled Rössler systems (11) when the coupling parameter value increases. If there is no phase synchronization between the oscillators, then their dynamics remain uncorrelated for all time scales s. Figure 5 illustrates the dynamics of two coupled Rössler systems when the coupling parameter ε is small enough ($\varepsilon = 0.025$). The power spectra $\langle E(s)\rangle$ of wavelet transform for Rössler systems differ from each other (Fig. 5,a), but the maximum values of the energy correspond approximately to the same time scale s in both systems. It is clear, that the phase difference $\phi_{s1}(t)-\phi_{s2}(t)$ is not bounded for almost all time scales (see Fig. 5,b). One can see that the phase difference $\varphi_{s1}(t) - \varphi_{s2}(t)$ increases for time scale $s = 3.0$, but decreases for $s = 4.5$. It means that there should be the time scale $3 < s^* < 4.5$ the phase difference on which remains bounded. This time scale s^* plays a role of a point separating the time scale areas with the phase difference increasing and decreasing, respectively. In this case the measure of time scales on which the phase difference remains bounded is zero and we can not say about the synchronous behavior of coupled chaotic oscillators (see also section V).

As soon as any of the time scales of the first chaotic oscillator becomes correlated with the other one of the second oscillator (e.g., when the coupling parameter increases), the phase synchronization occurs (see Fig. 4). The time scales s characterized by the largest value of energy in wavelet spectrum $\langle E(s)\rangle$ are more likely to become correlated first. The other time scales remain uncorrelated as before. The phase synchronization between chaotic oscillators leads to the phase locking (3) on the correlated time scales s.

When the parameter of coupling between chaotic oscillators increases, more and more time scales become correlated and one can say that the degree of the synchronization grows. So, with the further increasing of the coupling parameter value (e.g., $\varepsilon = 0.07$) in the coupled Rössler systems (11) the time scales which were uncorrelated before become synchronized (see Fig. 6,b). It is evident, that the time scales $s = 4.5$ are synchronized in comparison with the previous case ($\varepsilon = 0.05$, Fig. 4,b) when these time scales were uncorrelated. The number of time scales s demonstrating the phase locking increases, but there are nonsynchronized

time scales as before (e.g., the time scales $s = 3.0$ and $s = 6.0$ remain still nonsynchronized).

Arising of the lag synchronization [21] between oscillators means that all time scales are correlated. Indeed, from the condition of the lag–synchronization $x_1(t-\tau) \simeq x_2(t)$ one can obtain that $W_1(s, t-\tau) \simeq W_2(t, s)$ and therefore $\phi_{s1}(t-\tau) \simeq \phi_{s2}(t)$. It is clear, in this case the phase locking condition (3) is satisfied for all time scales s. For instance, when the coupling parameter of chaotic oscillators (11) becomes large enough ($s = 0.25$) the lag synchronization of two coupled oscillators appears. In this case the power spectra of wavelet transform coincide with each other (see Fig. 7,a) and the phase locking takes place for all time scales s (Fig. 7,b). It is important to note that the phase difference $\phi_{s1}(t) - \phi_{s2}(t)$ is not equal to zero for the case of the lag synchronization. It is clear that this difference depends on the time lag τ.

Further increasing of the coupling parameter leads to the decreasing of the time lag τ [21]. Both systems tend to have the complete synchronization regime $x_1(t) \simeq x_2(t)$, so the phase difference $\phi_{s1}(t) - \phi_{s2}(t)$ tends to be a zero for all time scales.

The dependence of synchronized time scale range $[s_m; s_b]$ on coupling parameter has been shown in Fig. 8. The range $[s_m; s_b]$ of synchronized time scales appears at $\varepsilon \approx 0.039$. The appearance of synchronized time scale range corresponds to the phase synchronization regime. When the coupling parameter value increases the range of synchronized time scales expands until all time scales become synchronized. Synchronization of all time scales means the presence of lag synchronization regime.

So, we can say the time scale synchronization (TSS) is the most general synchronization type uniting (at least) PS, LS and CS regimes.

IV. GENERALIZED SYNCHRONIZATION REGIME

Let us consider another type of synchronized behavior, so–called the generalized synchronization. It has been shown above, that PS, LS and CS are naturally interrelated with each other and the synchronization type depends on the number of synchronized time scales. The details of the relations between PS and GS is not at all clear. There are several works [1, 22] dealing with the problem, how GS and PS are correlated with each other. For instance, in [22] it has been reported that two unidirectional coupled Rössler systems can demonstrate the generalized synchronization while the phase synchronization has not been

observed. This case allows to be explained easily by means of the time scale analysis. The equations of Rössler system are

$$\begin{aligned}
\dot{x}_1 &= -\omega_1 y_1 - z_1,\\
\dot{y}_1 &= \omega_1 x_1 + a y_1,\\
\dot{z}_1 &= p + z_1(x_1 - c)\\
\dot{x}_2 &= -\omega_2 y_2 - z_2 + \varepsilon(x_1 - x_2),\\
\dot{y}_2 &= \omega_2 x_2 + a y_2,\\
\dot{z}_2 &= p + z_2(x_2 - c),
\end{aligned} \tag{12}$$

where $\mathbf{x}_1 = (x_1, y_1, z_1)^T$ and $\mathbf{x}_2 = (x_2, y_2, z_2)^T$ are the state vectors of the first (drive) and the second (response) Rössler systems, respectively. The control parameter values have been chosen as $\omega_1 = 0.8$, $\omega_2 = 1.0$, $a = 0.15$, $p = 0.2$, $c = 10$ and $\varepsilon = 0.2$. The generalized synchronization takes place in this case (see [22] for detail). Why it is impossible to detect the phase synchronization in the system (12) despite the generalized synchronization is observed becomes clear from the time scale analysis.

Let us consider Fourier spectra of coupled chaotic oscillators (see Fig. 9). There are two main spectral components with frequencies $f_1 = 0.125$ and $f_2 = 0.154$ in these spectra. The analysis of behavior of time scales has shown that both the time scales $s_1 = 1/f_1 = 8$ of coupled oscillators corresponding to the frequency f_1 and time scales close to s_1 are synchronized while the time scales $s_2 = 1/f_2 \simeq 6.5$ and close to them do not demonstrate synchronous behavior (Fig. 10,b).

The source of such behavior of time scales becomes clear from the wavelet power spectra $\langle E(s)\rangle$ of both systems (see Fig. 10,a). The time scale s_1 of the drive Rössler system is characterized by the large value of energy while the part of energy being fallen on this scale of the response system is quite small. Therefore, the drive system dictates its own dynamics on the time scale s_1 to the response system. The opposite situation takes place for the time scales s_2 (see Fig. 10,a). The drive system can not dictate its dynamics to the response system because the part of energy being fallen on this time scale is small in the first Rössler system and large enough in the second one. So, time scales s_2 are not synchronized.

Thus, the generalized synchronization of the unidirectional coupled Rössler systems appears as the time scale synchronized dynamics, as another synchronization types does before. It is also clear, why the phase synchronization has not been observed in this case. Fig. 9 shows that the instantaneous phases $\phi_{1,2}(t)$ of chaotic signals $\mathbf{x}_{1,2}(t)$ introduced by means of

traditional approaches are determined by both frequencies f_1 and f_2, but only the spectral components with the frequency f_1 are synchronized. So, the observation of instantaneous phases $\phi_{1,2}(t)$ does not allow to detect the phase synchronization in this case although the synchronization of time scales takes place.

Thus, one can see that there is a close relationship between different types of the chaotic oscillator synchronization. According to results mentioned above we can say that PS, LS, CS and GS are particular cases of TSS. Therefore, it is possible to consider different types of synchronized behavior from the universal position. Unfortunately, it is not clear, how one can distinguish the phase synchronization. (Here we mean the phase synchronization between chaotic oscillators takes place if the instantaneous phase $\phi(t)$ of chaotic signal may be correctly introduced by means of traditional approaches and the phase locking condition (1) is satisfied). and the generalized synchronization using only the results obtained from the analysis of the time scale dynamics.

V. MEASURE OF SYNCHRONIZATION

From examples mentioned above one can see that any type of synchronous behavior of coupled chaotic oscillators leads to arising of the synchronized time scales. Therefore, the measure of synchronization can be introduced. This measure ρ can be defined as the the part of wavelet spectrum energy being fallen on the synchronized time scales

$$\rho_{1,2} = \frac{1}{E_{1,2}} \int\limits_{s_m}^{s_b} \langle E_{1,2}(s) \rangle \, ds, \tag{13}$$

where $[s_m; s_b]$ is the range of time scales for which the condition (1) is satisfied and $E_{1,2}$ is a full energy of the wavelet spectrum

$$E_{1,2} = \int\limits_{0}^{+\infty} \langle E_{1,2}(s) \rangle \, ds. \tag{14}$$

This measure ρ is 0 for the nonsynchronized oscillations and 1 for the case of complete and lag synchronization regimes. If the phase synchronization regime is observed it takes a value between 0 and 1 depending on the part of energy being fallen on the synchronized time scales. So, the synchronization measure ρ allows not only to distinguish the synchronized and nonsynchronized oscillations, but characterize quantitatively the degree of TSS synchronization.

Fig. 11 presents the dependence of the TSS synchronization measure ρ_1 for the first Rössler oscillator of system (11) considered in section III on the coupling parameter ε. It is clear that the part of the energy being fallen on the synchronized time scales growths monotonically with the growth of the coupling strength. Similar results have been obtained for the generalized synchronization of two coupled Rössler systems considered in section IV.

It has already mentioned above that when the coupled oscillators do not demonstrate synchronous behavior there are time scales s^* the phase difference $\varphi_{s1}(t) - \varphi_{s2}(t)$ on which is bounded. Such time scales play role of points separating the time scale areas where the phase difference increases and decreases, respectively (see also section III). Nevertheless, the presence of such time scales does not mean the occurrence of chaotic synchronization because the part of energy being fallen on them is equal to zero. Therefore, the synchronization measure ρ of such oscillations is zero, and dynamical regime being realized in the system in this case should be classified as non-synchronous.

VI. CONCLUSION

Summarizing this work we would like to note several principal aspects. Firstly, we have proposed to consider the time scale dynamics of coupled chaotic oscillators. It allows us to consider the different types of behavior of coupled oscillators (such as the complete synchronization, the lag synchronization, the phase synchronization, the generalized synchronization and the nonsynchronized oscillations) from the universal position. In this case TSS is the most common type of synchronous coupled chaotic oscillator behavior. Therefore, the another types of synchronous oscillations (PS, LS, CS and GS) may be considered as the particular cases of TSS. The quantitative characteristic ρ of the synchronization measure has also been introduced. It is important to note that our method (with insignificant modifications) can also be applied to dynamical systems synchronized by the external (e.g., harmonic) signal.

Secondly, the traditional approach for the phase synchronization detecting based on the introducing of the instantaneous phase $\phi(t)$ of chaotic signal is suitable and correct for such time series characterized by the Fourier spectrum with the single main frequency f_0. In this case the phase ϕ_{s0} associated with the time scale s_0 corresponding to the main frequency f_0 of the Fourier spectrum coincides approximately with the instantaneous phase $\phi(t)$ of

chaotic signal introduced by means of the traditional approaches (see also [36]). Indeed, as the other frequencies (the other time scales) do not play a significant role in the Fourier spectrum, the phase $\phi(t)$ of chaotic signal is close to the phase $\phi_{s0}(t)$ of the main spectral frequency f_0 (and the main time scale s_0, respectively). It is obvious, that in this case the mean frequencies $\bar{f} = \langle\dot{\phi}(t)\rangle/2\pi$ and $\bar{f}_{s0} = \langle\dot{\phi}_{s0}(t)\rangle/2\pi$ should coincide with each other and with the main frequency f_0 of the Fourier spectrum (see also [31])

$$\bar{f} = \bar{f}_{s0} = f_0. \tag{15}$$

If the chaotic time series is characterized by the Fourier spectrum without the main single frequency (like the spectrum shown in the Fig. 3,*b*) the traditional approaches fail. One has to consider the dynamics of the system on all time scales, but it is impossible to do it by means of the instantaneous phase $\phi(t)$. On the contrary, our approach based on the time scale dynamics analysis can be used for both types of chaotic signals.

Finally, our approach can be easily applied to the experimental data because it does not require any a-priori information about the considered dynamical systems. Moreover, in several cases the influence of the noise can be reduced by means of the wavelet transform (for detail, see [39, 48, 49]). We believe that our approach will be useful and effective for the analysis of physical, biological, physiological and other data, such as [10, 35, 36].

Acknowledgments

We express our appreciation to Corresponding Member of Russian Academy of Science, Professor Dmitriy I. Trubetskov and Professors Vadim S. Anishchenko and Tatyana E. Vadivasova for valuable discussions. We also thank Svetlana V. Eremina for the support.

This work has been supported by U.S. Civilian Research & Development Foundation for the Independent States of the Former Soviet Union (CRDF), grant REC–006 and Russian Fundation for Basic Research, Grant 02–02–16351. A.E.H. also thanks "Dynastiya" Foundation.

[1] Parlitz U., Junge L., Lauterborn W., Phys. Rev. E **54**, 2115 (1996).

[2] Tang D.Y., Dykstra R., Hamilton M.W., Heckenberg N.R., Phys. Rev. E **57**, 3649 (1998).

[3] Allaria E., Arecchi F.T., Garbo A.D., Meucci R., Phys. Rev. Lett. **86**, 791 (2001).

[4] Ticos C.M., Rosa E., Pardo W.B., Walkenstein J.A., Monti M., Phys. Rev. Lett. **85**, 2929 (2000).

[5] Rosa E., Pardo W.B., Ticos C.M., Wakenstein J.A.,Monti M., Int. J. Bifurcation and Chaos **10**, 2551 (2000).

[6] Trubetskov D.I., Hramov A.E., Journal of Communications Technology and Electronics **48**, 105 (2003).

[7] Tass P.A. at al., Phys. Rev. Lett. **81**, 3291 (1998).

[8] Anishchenko V.S., Balanov A.G., Janson N.B., Igosheva N.B., Bordyugov G.V., Int. J. Bifurcation and Chaos **10**, 2339 (2000).

[9] Prokhorov at al., Phys. Rev. E **68**, 041913 (2003).

[10] Elson R.C. at al., Phys. Rev. Lett. **81**, 5692 (1998).

[11] Rulkov N.F., Phys. Rev. E **65**, 041922 (2002).

[12] Tass P.A. et al., Phys. Rev. Lett. **90**, 088101 (2003).

[13] Pikovsky A., Rosenblum M., Kurths J., *Synchronization: a universal concept in nonlinear sciences* (Cambridge University Press, 2001).

[14] Pikovsky A., Rosenblum M., Kurths J., Int. J. Bifurcation and Chaos **10**, 2291 (2000).

[15] Anishchenko V.S., Vadivasova T.E., Journal of Communications Technology and Electronics **47**, 117 (2002).

[16] Anshchenko V.S., Astakhov V., Neiman A., Vadivasova T.,Schimansky-Geier L., *Nonlinear Dynamics of Chaotic and Stochastic Systems. Tutorial and Modern Developments* (Springer–Verlag, Heidelberg, 2001).

[17] Pecora L.M., Carroll T.L., Phys. Rev. Lett. **64**, 821 (1990).

[18] Pecora L.M., Carroll T.L., Phys. Rev. A **44**, 2374 (1991).

[19] Murali K., Lakshmanan M., Phys. Rev. E **49**, 4882 (1994).

[20] Murali K., Lakshmanan M., Phys. Rev. E **48**, R1624 (1994).

[21] Rosenblum M.G., Pikovsky A.S., Kurths J., Phys. Rev. Lett. **78**, 4193 (1997).

[22] Zheng Z., Hu G., Phys. Rev. E **62**, 7882 (2000).

[23] Taherion S., Lai Y.C., Phys. Rev. E **59**, R6247 (1999).

[24] Rulkov N.F., Sushchik M.M., Tsimring L.S., Abarbanel H.D.I., Phys. Rev. E **51**, 980 (1995).

[25] Kocarev L., Parlitz U., Phys. Rev. Lett. **76**, 1816 (1996).

[26] Pyragas K., Phys. Rev. E **54**, R4508 (1996).

[27] Rosenblum M.G., Pikovsky A.S., Kurths J., Phys. Rev. Lett. **76**, 1804 (1996).

[28] Osipov G.V., Pikovsky A.S., Rosenblum M.G., Kurth J., Phys. Rev. E **55**, 2353 (1997).

[29] Abarbanel H.D.I., Rulkov N.F., Sushchik M., Phys. Rev. E **53**, 4528 (1996).

[30] Pecora L.M., Carroll T.L., Heagy J.F., Phys. Rev. E **52**, 3420 (1995).

[31] Anishchenko V.S., Vadivasova T.E., Journal of Communications Technology and Electronics **49**, 69 (2004).

[32] Pikovsky A., Rosenblum M., Osipov G., Kurths J., Physica D **104**, 219 (1997).

[33] Rosenblum M.G. et al., Phys. Rev. Lett. **89**, 264102 (2002).

[34] Osipov G.V. at al., Phys. Rev. Lett. **91**, 024101 (2003).

[35] Lachaux J.P. et al., Int. J. Bifurcation and Chaos **10**, 2429 (2000).

[36] Quiroga R.Q., Kraskov A., Kreuz T., Grassberger P., Phys. Rev. E **65**, 041903 (2002).

[37] Pikovsky A.S., Rosenblum M.G., Kurths J., Europhysics Letters **34**, 165 (1996).

[38] Koronovskii A.A., Hramov A.E., JETP Letters **79**, 316 (2004).

[39] Koronovskii A.A., Hramov A.E., *Continuous wavelet analysis and its applications (In Russian)* (Moscow, Fizmatlit, 2003).

[40] Daubechies I., *Ten lectures on wavelets* (SIAM, 1992).

[41] Kaiser G., *A friendly guide to wavelets* (Springer Verlag, 1994).

[42] Torresani B., *Continuous wavelet transform* (Paris: Savoire, 1995).

[43] Lachaux J.P. et al., Neurophysiol. Clin. **32**, 157 (2002).

[44] Quyen M.L.V. at al., J. Neuroscience Methods **111**, 83 (2001).

[45] DeShazer D.J., Breban R., Ott E., Roy R., Phys. Rev. Lett. **87**, 044101 (2001).

[46] Sosnovtseva O.V., Pavlov A.N., Mosekilde E., Holstein-Rathlou N.-H., Phys. Rev. E **66**, 061909 (2002).

[47] Grossman A. and Morlet J., SIAM J. Math. Anal. **15**, 273 (1984).

[48] Torrence C., Compo G.P., Bulletin of the American Meteorological Society **79**, 61 (1998).

[49] Gusev V.A., Koronovskiy A.A., Hramov A.E., Technical Physics Letters **29**, 61 (2003).

CAPTIONS

Fig. 1. (a) Phase coherent attractor and (b) spectrum of the first Rössler system (10). Coupling parameter ε between oscillators is equal to zero

Fig. 2. (a) Wavelet power spectrum $\langle E(s)\rangle$ for the first (solid line) and the second (dashed line) Rössler systems (10). (b) The dependence of phase difference $\phi_{s1}(t)-\phi_{s2}(t)$ on time t for different time scales s. The coupling parameter between oscillators is $\varepsilon=0.05$. The phase synchronization for two coupled chaotic oscillators is observed

Fig. 3. (a) Phase picture and (b) power spectrum of the first Rössler system (11) oscillations. Coupling parameter ε is equal to zero

Fig. 4. (a) The normalized energy distribution in wavelet spectrum $\langle E(s)\rangle$ for the first (the solid line denoted "1") and the second (the dashed line denoted "2") Rössler systems (11); (b) the phase difference $\phi_{s1}(t)-\phi_{s2}(t)$ for two coupled Rössler systems. The value of coupling parameter has been selected as $\varepsilon=0.05$. The time scales $s=5.25$ are correlated with each other and the synchronization has been observed

Fig. 5. (a) The normalized energy distribution in wavelet spectrum $\langle E(s)\rangle$ for the first (the solid line denoted "1") and the second (the dashed line denoted "2") Rössler systems; (b) the phase difference $\phi_{s1}(t)-\phi_{s2}(t)$ for two coupled Rössler systems. The value of coupling parameter has been selected as $\varepsilon=0.025$. There is no phase synchronization between systems

Fig. 6. (a) The normalized energy distribution in wavelet spectrum $\langle E(s)\rangle$ for the first (the solid line denoted "1") and the second (the dashed line denoted "2") Rössler systems; (b) the phase difference $\phi_{s1}(t)-\phi_{s2}(t)$ for two coupled Rössler systems. The value of coupling parameter has been selected as $\varepsilon=0.07$.

Fig. 7. (a) The normalized energy distribution in wavelet spectrum $\langle E(s)\rangle$ for the Rössler system; (b) the phase difference $\phi_{s1}(t)-\phi_{s2}(t)$ for two coupled Rössler systems. The value of coupling parameter has been selected as $\varepsilon=0.25$. The lag synchronization has been observed, all time scales are synchronized

Fig. 8. The dependence of the synchronized time scale range $[s_m;s_b]$ on the coupling strength ε for two mutually coupled Rössler systems (11) with funnel attractors

Fig. 9. Fourier spectra for(a) the first (drive) and (b) the second (response) Rösler systems (12). The coupling parameter is $\varepsilon = 0.2$. The generalized synchronization takes place

Fig. 10. (a) The normalized energy distribution in wavelet spectrum $\langle E(s)\rangle$ for the first (the solid line denoted "1") and the second (the dashed line denoted "2") Rössler systems. The time scales pointed with arrows correspond to the frequencies $f_1 = 0.125$ and $f_2 = 0.154$, respectively; (b) the phase difference $\phi_{s1}(t) - \phi_{s2}(t)$ for two coupled Rössler systems. The generalized synchronization has been observed

Fig. 11. The dependence of the synchronization measure ρ_1 for the first Rössler system (11) on the coupling strength ε. The measure ρ_2 for the second Rössler oscillator behaves in a similar manner, so it has not been shown in the figure

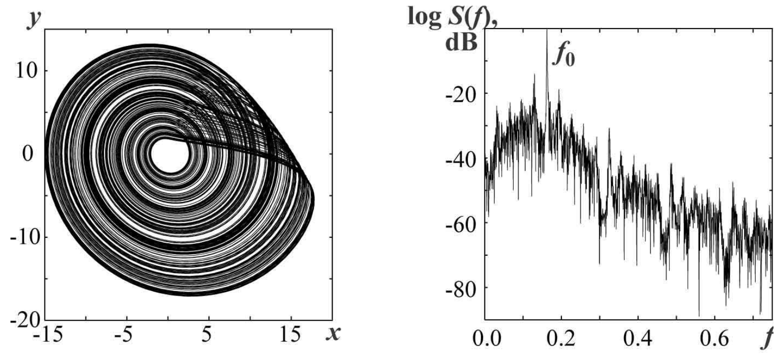

a *b*

FIG. 1:

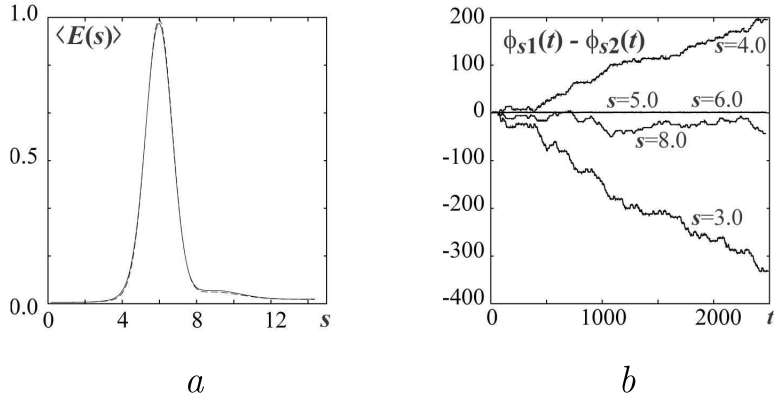
⟨E(s)⟩
1.0
0.5
0.0
0
4
8
12
s
a
φs1(t) - φs2(t)
200
100
0
-100
-200
-300
-400
0
1000
2000
t
s=4.0
s=5.0
s=6.0
s=8.0
s=3.0
b

FIG. 2:

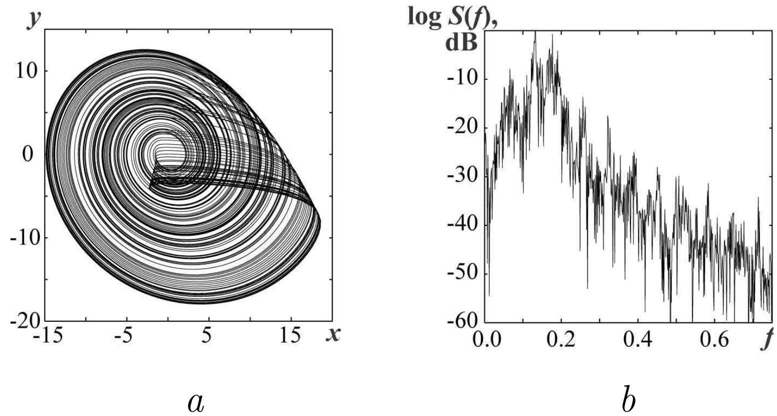

FIG. 3:

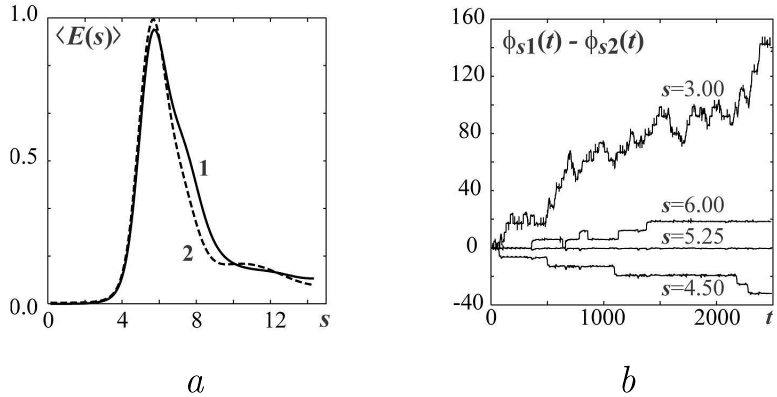

1.0
⟨E(s)⟩
0.5
1
2
0.0
0
4
8
12
s
a
160
$\phi_{s1}(t)$ - $\phi_{s2}(t)$
120
s=3.00
80
40
s=6.00
0
s=5.25
s=4.50
-40
0
1000
2000
t
b

FIG. 4:

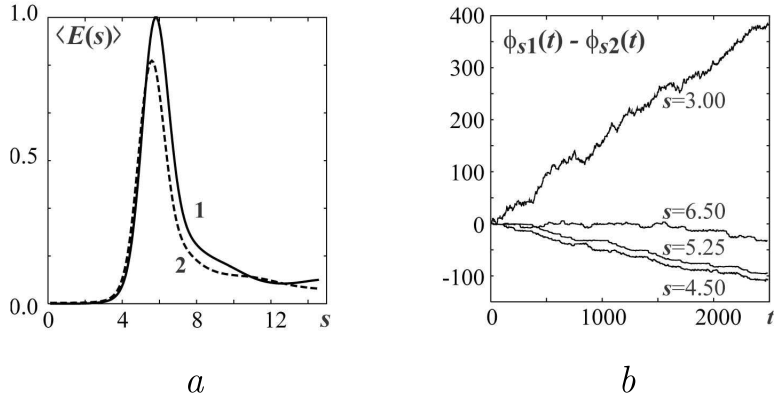

1.0
0.5
0.0
⟨E(s)⟩
1
2
0
4
8
12
s
a
400
300
200
100
0
-100
ϕs1(t) - ϕs2(t)
s=3.00
s=6.50
s=5.25
s=4.50
0
1000
2000
t
b

FIG. 5:

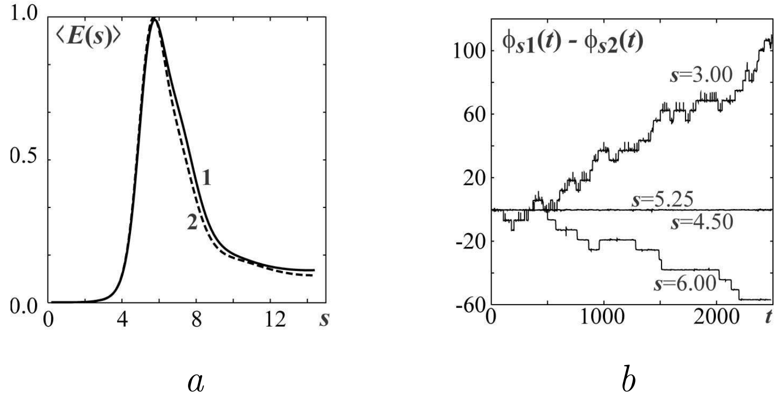

1.0
0.5
0.0
⟨E(s)⟩
1
2
0
4
8
12
s
a
100
60
20
-20
-60
φs1(t) - φs2(t)
s=3.00
s=5.25
s=4.50
s=6.00
0
1000
2000
t
b

FIG. 6:

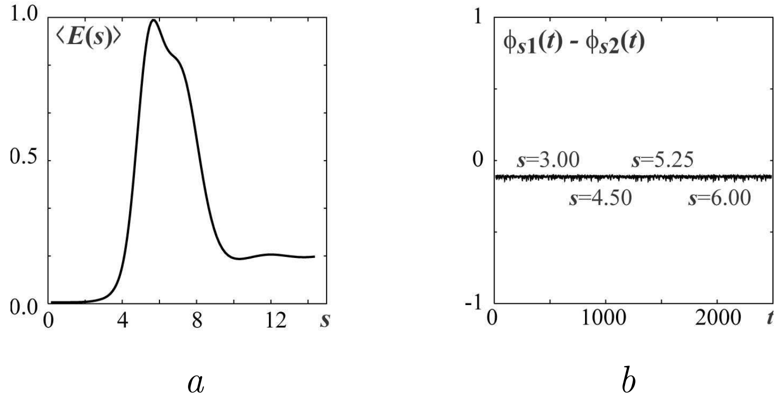

1.0
0.5
0.0
⟨E(s)⟩
0
4
8
12
s
a
1
0
-1
ϕs1(t) - ϕs2(t)
s=3.00
s=5.25
s=4.50
s=6.00
0
1000
2000
t
b

FIG. 7:

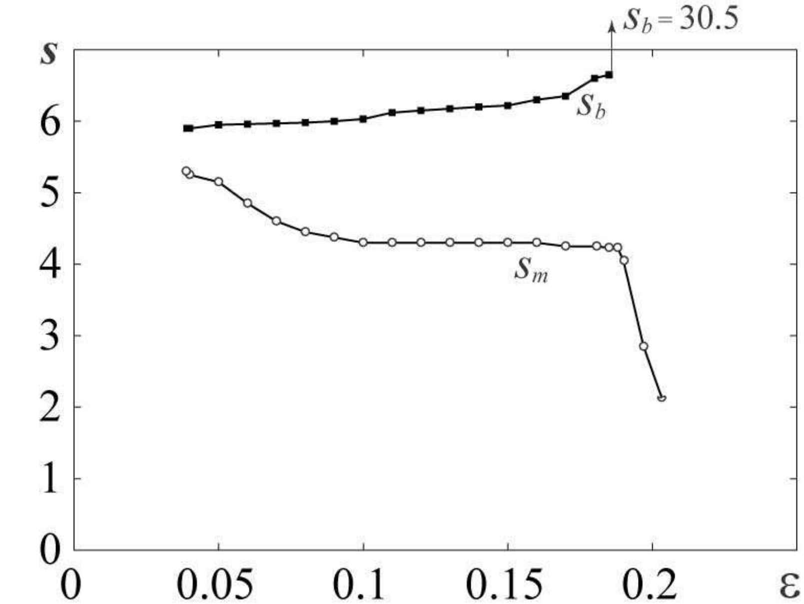

FIG. 8:

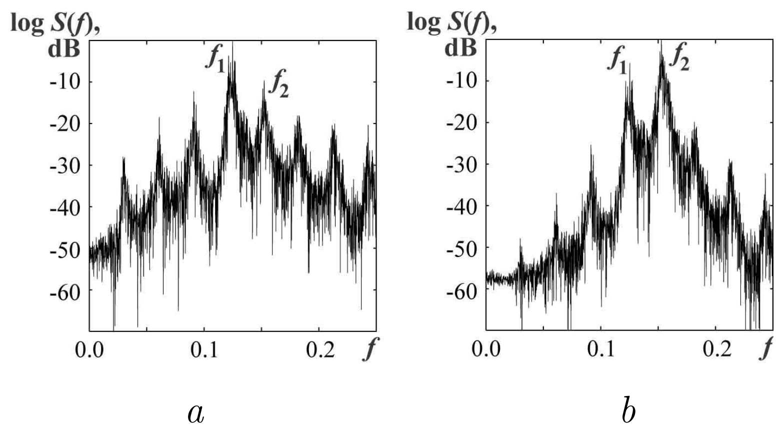
log S(f),
dB
-10
-20
-30
-40
-50
-60
0.0
0.1
0.2
f
f1
f2
a
log S(f),
dB
-10
-20
-30
-40
-50
-60
0.0
0.1
0.2
f
f1
f2
b

FIG. 9:

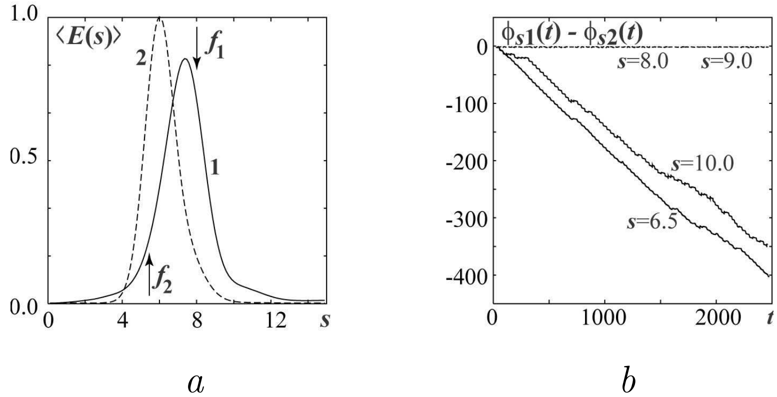
⟨E(s)⟩
1.0
0.5
0.0
2
1
f_1
f_2
0
4
8
12
s
$\phi_{s1}(t) - \phi_{s2}(t)$
0
-100
-200
-300
-400
s=8.0
s=9.0
s=10.0
s=6.5
0
1000
2000
t
a
b

FIG. 10:

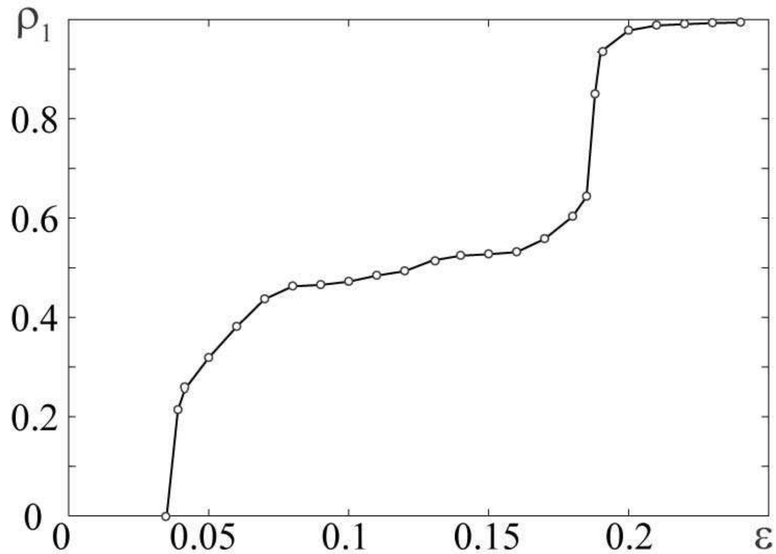

FIG. 11: